

立即咬合受力之人工牙根的研發與生物力學分析

Development and biomechanical analysis of immediately loaded implant

計畫編號：NSC 98-2320-B-039-005-MY3

執行期間：2009年8月1日至2012年7月31日

黃恆立(Heng-Li Huang)¹ 陳遠謙(Michael YC Chen)^{1,2} 林殿傑(Lin Dan-Jae)³

¹中國醫藥大學附設醫院 牙科部 (Department of Dentistry, China Medical University Hospital)

²中國醫藥大學 牙醫系 (School of Dentistry, China Medical University)

³中國醫藥大學 口腔衛生學系 (Department of Dental Hygiene, China Medical University)

一、中文摘要

本三年的研究計畫針對立即咬合植牙進行了三個主題的探討。第一個主題，本研究結合逆向工程-快速原型技術與有線元素分析探討下顎後牙區立即咬合人工植牙的生物力學行為(包含植體周圍骨質應力、植體與骨質之間的介面滑移量)。第二個主題，本研究分析立即咬合受力人工牙根在不同緻密骨厚度與鬆質骨強度下，其人工牙根初始穩定度與周圍骨質的受力(e.g. 應變)的影響。第三個主題，本研究探討進行人工植牙前，於骨缺損處以自體骨粉為填補骨材，以微米級電腦斷層掃描分析骨重塑後，移植骨與其周邊的顎骨骨質，兩者在骨礦化密度與三維骨小梁的結構，是否具有差異？此外，本研究亦探討骨重塑後，性別是否會影響移植骨骨質之骨礦化密度與三維骨小梁的結構？本研究計劃的執行將對立即咬合植牙之人工牙根，其生物力學與周圍骨質狀況，已有一清楚的瞭解，給予臨床醫師進行相關人工植牙的術前評估。此外，本研究計劃提供之研究成果，對國內之醫療植體之設計與發展，應可提供實質上的貢獻。

關鍵詞：立即咬合植牙、有限元素分析、骨質應力(應變)、人工牙根-骨質之間的介面滑移量、緻密骨厚度、鬆質骨強度、人工牙根初始穩定度、微米級電腦斷層掃描、自體骨粉、骨礦化密度、三維骨小梁的結構。

Abstract

There are three topics in this 3 years research project. Firstly, Experiment with rapid prototyping technique and validation finite element model were performed to evaluate the biomechanical behavior (including bone stress and interfacial sliding between implant and bone) of an immediately loaded mandibular implant. Secondly, the effects of cortical bone thickness and trabecular bone elastic

modulus on the strain in the bone surrounding an immediately loaded implant were evaluated. Thirdly, this research project used micro-level computed tomography (Micro-CT) investigated the effects of gender on the three-dimensional (3D) bone mineral density (BMD) and micromorphology of the trabeculae of matured autogenous bone grafts after sinus floor augmentation, and compared them to those of adjacent native bone. The execution of the research program present the clear understandings related to biomechanical mechanism of immediate loading of implant especially for its' surrounding bone (at bone strain, bone density, and trabecular structure). These information might provide the guide for clinician; moreover, there might provide some contributions to the medical industry for the development of the medical implant.

Keywords: immediately loaded implant, finite element model, bone stress (strain), the sliding at the bone-implant interface, cortical bone thickness, trabecular bone elastic modulus, initial implant stability, Micro-CT, autogenous bone grafts, bone mineral density (BMD), micromorphology of the trabeculae.

二、目的

There are three research topics for the second year of this research plan.

Topic I. [*Biomechanical simulation of various surface roughnesses and geometric designs on an immediate-load dental implant*]; The present study compared the biomechanical effects of immediately loaded implants with various designs of implant shapes and designs of surface textures with different roughnesses in the edentulous mandible. Prior to osseointegration, the interface condition between the immediately loaded implant and bone is contact only and the interfacial micromotion between immediately loaded implant and bone can occur and influences the quality of osseointegration. Therefore, finite element (FE) modeling of nonlinear contact

was used to simulate the contact interfaces between the immediately loaded implant and bone, and the interfacial sliding at BII was evaluated. Moreover, immediately loaded implants were subjected to in-vitro experiments to validate the accuracy of the nonlinear FE model that incorporated human mandible geometry.

Topic II. [*Initial stability and bone strain evaluation of the immediately loaded dental implant: an in vitro model study*]; this study applied strain-gauge analysis to artificial bone samples to investigate how the biomechanical performance (e.g., bone strain) is related to the precise characteristics of bone quality and quantity—including the thickness of cortical bone and the elastic modulus of trabecular bone—of an immediately loaded implant. In addition, the relationships of the primary implant stability with the cortical–bone thickness and the elastic modulus of trabecular bone were examined by measuring the implant stability quotient (ISQ), ITV, and PTV.

Topic III. [*Micro-Computed tomography analysis of particular autogenous bone graft in sinus augmentation at 5 months: Differences on bone mineral density and 3D trabecular structure*]; the purpose of this topic was to investigate the relationship between micro-CT measurement parameters describing BMD and 3D microtrabecular indexes in autogenous bone graft and its adjacent native bone after a healing period following maxillary sinus bone grafting. In addition, to investigate the gender differences (if any) in bone mineral density (BMD) and 3D trabecular architecture of grafted bone, especially for older patients is also the goal of this topic.

三、材料與方法

Due to the limitation of the pages, the matter of the material and methods of these three topic can be referred to the articles [1]、[2]、[3].

四、結果與討論

Topic 1. [*Biomechanical simulation of various surface roughnesses and geometric designs on an immediate-load dental implant*]

The von-Mises stress distributions in cortical bone showed that the stresses were highest at the crestal region around the implant; otherwise, the high bone stresses were found near the valley of the threads, the apex of the implant, and the stepped areas where the implant's diameter changed in the stepped implant (Fig. 1). The stress in the bone around the immediately loaded implant was considerably higher

for lateral loading than for vertical loading (Fig. 2 a). The stresses in cortical bone (144.9 MPa) and trabecular bone (20.8 MPa) were highest in the cylindrical and stepped implants, respectively. The stresses in bone were more than 20% higher when using the stepped implant in the lateral loading mode, but they were at least 15% lower than those in the cylindrical implant (Fig. 2). In general, bone stresses were lower in threaded implants than in cylindrical and stepped implants (Fig. 2). The stress in trabecular bone and the sliding at the BII were 17–25% and 16–48% lower in the rectangular threaded implant than in the v-thread implant, respectively (Fig. 2b). The stress in cortical bone did not appear to differ between the tapered body and the straight body of threaded implants (with same rectangular thread). However, the stress in trabecular bone was 15–25% higher in the tapered body of threaded implant than in the straight body of threaded implant (Fig. 3a). However, the stress in cortical bone in the tapered body of threaded implant increased (by less than 15%) during vertical loading but decreased (by less 10%) during lateral loading except in the models with $\mu = 0.4$ (Fig. 2). The stresses in cortical bone did not differ in the implant with two thread sizes. Nevertheless, the peak stress in trabecular bone was about 15% lower in the implant with two thread sizes than in the v-thread implant with $\mu = 0.4$ (Fig. 3a). Increasing the frictional coefficient of the BII in the cylindrical implant and stepped implant increased the stress in cortical bone and reduced the stress in trabecular bone, but in the threaded implant this did not always increase the stress in cortical bone but clearly decreased the stress in trabecular bone (Figs. 2b and 3b).

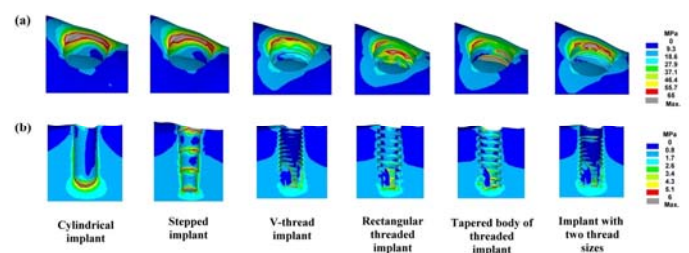


Fig. 1. von-Mises stress distributions in cortical bone (a) and trabecular bone (b) in models with $\mu = 0.4$ at the BII under lateral loading.

The sliding at the BII peaked (at 41.3 μm) in the cylindrical implant at the crestal region (Fig. 4) during vertical loading (Fig 5a). Otherwise, a high degree of sliding was also observed at the apex of implant and at the threads near the apex of the implant (Fig. 4). Sliding at the BII in both cylindrical and stepped implants (Fig. 5b) was at least 20% lower for the Al_2O_3 -blasted implant

surface ($\mu = 0.68$) than for the polished implant surface ($\mu = 0.4$). Likewise, sliding at the BII was more than 35% lower for the plasma sprayed ($\mu = 1.0$) and beaded porous ($\mu = 1.0$) implant surfaces (Fig. 5b). Threading the implant surface obviously reduced the interfacial sliding at the BII (Fig. 5a) during both vertical and lateral loading. Increasing μ from 0.4 to 0.68 and from 0.4 to 1.0 decreased sliding at the BII in threaded implants by 10–28% and 16–45%, respectively. Sliding at the BII was 16–50% lower in the square-shape threaded implant than in the v-thread implant. Using a tapered body design slightly increased sliding at the BII (especially during lateral loading) relative to a rectangular threaded implant (straight-body design). Reducing the thread pitch in cortical bone did not significantly affect sliding at the BII relative to the v-thread implant (Fig. 5).

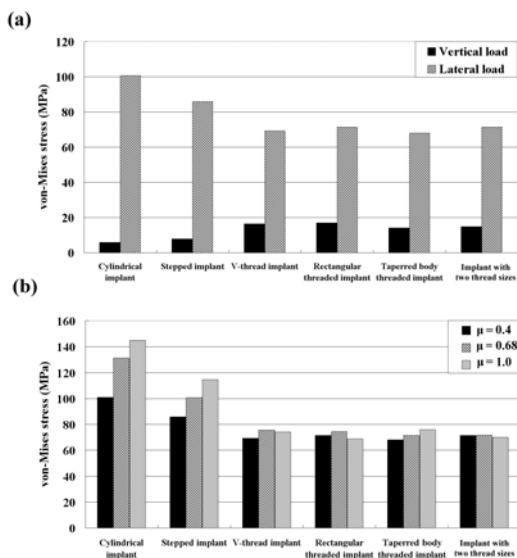


Fig. 2. Peak von-Mises stresses in cortical bone in models with $\mu = 0.4$ at the BII under vertical and lateral loadings (a), and in models with $\mu = 0.4, 0.68$, and 1.0 at the BII only under lateral loading (b).

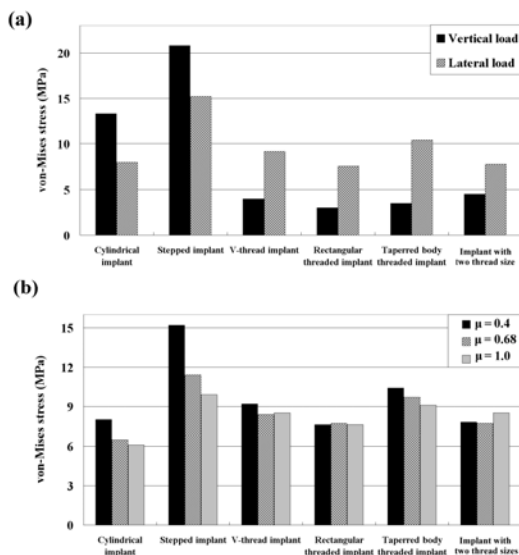


Fig. 3. Peak von-Mises stresses in trabecular bone in all models with $\mu = 0.4$ at the BII under vertical and lateral loadings (a), and in models with $\mu = 0.4, 0.68$, and 1.0 at the BII only under lateral loading (b).

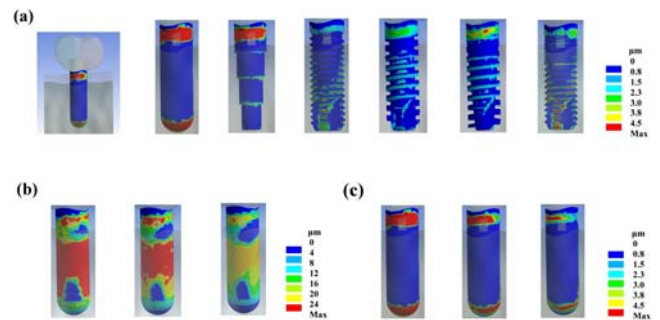


Fig. 4. Distributions of sliding at the BII in 6 implant models with $\mu = 0.4$ under lateral loading (a), and in cylindrical implants with $\mu = 0.4, 0.68$, and 1.0 (left to right, respectively) under vertical loading (b) and lateral loading (c).

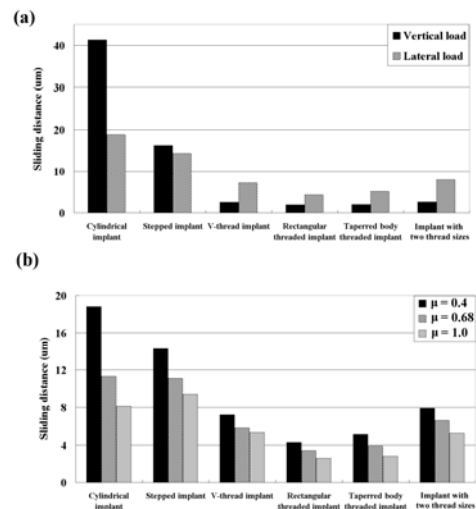


Fig. 5. Peak sliding at the BII in models with $\mu = 0.4$ under vertical and lateral loadings (a), and in models with $\mu = 0.4, 0.68$, and 1.0 only under lateral loading (b).

Topic II. [Initial stability and bone strain evaluation of the immediately loaded dental implant: an in vitro model study]

Peak strains in bone (minimum principal strains) around immediately loaded implants were at least twofold higher for lateral loading than for vertical loading. The peak bone strains differed significantly between the models with cortical bone thicknesses of 1, 2, and 3 mm in both Kruskal-Wallis test and Multiple comparison with Bonferroni test ($p < 0.05$) (Table 1). The bone strains in the model with a 1-mm-thick cortical bone were 10.3% and 52.1% higher than those in models with 2- and 3-mm-thick cortical bone, respectively, for vertical loading (Fig. 4a), and 35.0% and 62.0% for lateral loading.

The highest strain values (minimum principal strains) differed significantly between the models with trabecular bone with elastic moduli of 12.4, 23, 47.5, and 137 MPa in Kruskal-Wallis test and Multiple comparison with Bonferroni test ($p < 0.05$) (Table 2). For vertical loading the bone strain was 39.0%, 49.1%, and 73.1% higher in the model with 12.4-MPa trabecular bone than those with 23-, 47.5-, and 137-MPa trabecular bone, respectively; the corresponding differences for lateral loading were 42.4%, 44.0%, and 56.2% .

ITV, ISQ, and PTV all varied significantly with the thickness of cortical bone in Kruskal-Wallis test ($p \leq 0.05$): ITV rose increasingly while ISQ rose decreasingly when the thickness of cortical bone increased (Table 3). In addition, PTV was reduced decreasingly when cortical bone was thicker (Table 3).

ISQ and PTV varied significantly with the elastic modulus of trabecular bone in Kruskal-Wallis test ($p < 0.05$) (Table 4)

Due to the limitation of the pages, the detail of information related to Table 1, Table 2, Table 3, and Table 4 can be referred to the article [2].

Topic III. [*Micro-Computed tomography analysis of particular autogenous bone graft in sinus augmentation at 5 months: Differences on bone mineral density and 3D trabecular structure*]

The mean and standard deviation values of all of the measured parameters for both the grafted and native bone are listed in Table 5. Significant differences between the two bone types were observed for only three parameters: BV/TV, Tb.Th, and Tb.Pf ($P < 0.05$). BV/TV and Tb.Th was 35.5% and 37.7% greater for native bone than for grafted bone respectively, while Tb.Pf was lower for native bone [0.07 (1/pixel)] than for grafted bone [0.19 (1/pixel)]. Since significant outcomes were found for only BV/TV, Tb.Th, and Tb.Pf ($P < 0.05$), correlations of BV/TV, Tb.Th, and Tb.Pf between the grafted and native bone are shown in Fig.6. A weakly positive correlation was found between the Tb.Th values of grafted and native bone ($R^2=0.58$), while no apparent correlation was found for BV/TV ($R^2=0.31$) and Tb.Pf ($R^2=0.15$) between the two bone types.

Table 6 details the differences in trabecular BMD and 3D architecture in grafted bone and the adjacent native bone between males and females. With the exception of SMI in native bone, there were no significant gender-specific differences in either BMD or 3D trabecular structure for the two bone types ($P > 0.05$).

Due to the limitation of the pages, the detail of

information related to Table 5, Table 6, and Fig. can be referred to the article [3].

四、結論

Topic 1. [*Biomechanical simulation of various surface roughnesses and geometric designs on an immediate-load dental implant*]

1. Adding threading to an implant can significantly decrease the bone stress and sliding at the BII relative to nonthreaded implants (in cylindrical and stepped implants).
2. The stress in trabecular bone and sliding at the BII are lower for the rectangular threaded implant than for the v-thread implant. Using shorter threads in cortical bone decreases sliding at the BII but not bone stresses.
3. The stress reduction in cortical bone and sliding at the BII does not differ significantly between threaded implants with tapered and straight bodies, and stresses in trabecular bone are higher in the tapered body of threaded implant.
4. It is not purely advantageous for the implant surface texture to have a high roughness (such as produced by plasma spraying or a beaded porous surface), since this decreases sliding at the BII it increases the crestal bone stress around the implant.

Topic II. [*Initial stability and bone strain evaluation of the immediately loaded dental implant: an in vitro model study*]

5. The strains induced in bone around an immediately loaded implant are at least twofold higher for lateral loading than for vertical loading.
6. In the presence of thin cortical bone and/or weak trabecular bone, immediate implant loading induces large bone strains and might increase the risk of implant failure. Bone strain can be reduced by placing an immediately loaded implant in thicker cortical bone and/or in trabecular bone with a denser structure. In addition, the relationship between bone strain and the strength of trabecular bone is nonlinear. The bone strain is increased more by decreasing the strength of softer trabecular bone than of denser trabecular bone.
7. In second-order regression the cortical bone thickness and strength of trabecular bone were strongly correlated with ITV, ISQ, and PTV (all $R^2 > 0.9$). The effect of cortical bone thickness increased for ITV but decreased for ISQ and PTV when cortical bone is thicker. Moreover, as the strength of trabecular bone increased, the increase in ITV became linear.

Topic III. [*Micro-Computed tomography analysis of particular autogenous bone graft in sinus augmentation at 5 months: Differences on bone mineral density and 3D trabecular structure*]

8. BV/TV, Tb.Th, and the connectivity of the trabeculae (i.e., Tb.Pf) are both lower in grafted than native bone. There is a weak positive correlation in Tb.Th values between native bone and grafted bone.
9. The BMDs and 3D trabecular structures of native bone and grafted bone do not differ significantly with gender.

五、參考文獻

- [1] H. L. Huang, J.T. Hsu, L.J. Fuh, D.J. Lin, M. Y.C. Chen, “Biomechanical Simulation of Various Surface Roughnesses and Geometric Designs on an Immediately Loaded Dental Implant”, *Comput. Biol. Med.*, 40:525-532, 2010.
- [2] H.L. Huang, Y.Y. Chang, D.J. Lin, Y.F. Li, K.T. Chen, J.T. Hsu, “Initial stability and bone strain evaluation of the immediately loaded dental implant: an in vitro study”, *Clin. Oral Implants Res.*, 22: 691-698, 2011.
- [3] H.L. Huang, J.T. Hsu, M.Y.C. Chen, C. Liu, C.H. Chang, Y.F. Li, K.T. Chen, “Micro-Computed tomography analysis of particular autogenous bone graft in sinus augmentation at 5 months: Differences on bone mineral density and 3D trabecular structure”, *Clin. Oral Invest.*, early view & in-press, 2012.